3D+t Brain MRI Segmentation Using Robust 4D Hidden Markov Chain

François Lavigne, Christophe Collet and Jean-Paul Armspach

***Abstract*— In recent years many automatic methods have been developed to help physicians diagnose brain disorders, but the problem remains complex. In this paper we propose a method to segment brain structures on two 3D multi-modal MR images taken at different times (longitudinal acquisition). A bias field correction is performed with an adaptation of the Hidden Markov Chain (HMC) allowing us to take into account the temporal correlation in addition to spatial neighbourhood information. To improve the robustness of the segmentation of the principal brain structures and to detect Multiple Sclerosis Lesions as outliers the Trimmed Likelihood Estimator (TLE) is used during the process. The method is validated on 3D+t brain MR images.**

I. INTRODUCTION

Magnetic Resonance Imaging (MRI) is widely used for brain evolutive disorders diagnosis as Multiple sclerosis (MS) or Alzheimer's disease. The segmentation of the brain structures and the analysis of their evolutions are crucial steps in these diseases diagnosis. Automated methods have been developed to help physicians (manual process is always too much time consuming) [1]. For the special case of the segmentation of MS lesions, more details can be found in [2] and [3].

In this paper we propose a method for segmentation into 3 classes the brain structures (White Matter (WM), Grey Matter (GM) and Cerebrospinal Fluid (CSF)) taking into account their evolutions. We simultaneously segment two 3D multi-modal MR images taken at two different times using an Hidden Markov Chain (HMC) model. The use of the HMC model allows to take both spatial and temporal neighbourhood information in order to introduce a spatio-temporal regularization during the segmentation process. This will reduce the influence of the noise in the MR images and will take simultaneously into account time evolution. The criteria of segmentation and the parameters of the HMC model are automatically estimated by using the Baum-Welch algorithm [4], highly reducing the computation time compared to Markov Random Field. In the used data, there are always artefacts due to MR images by themselves or due to studied diseases (for example in MS, lesions differ from the three looked brain structures). To reduce this artefacts and improve the robustness, the data driven term is estimated by using the Trimmed Likelihood Estimator method. Moreover the methods allow to dtermine outliers from the 3 classes model. After a post-treament, the MS lesions are segmented using this outliers.

F. Lavigne, C Collet and J.-P. Armspach are with the University of Strasbourg - CNRS, ICube Lab., contacts: f.lavigne@unistra.fr, c.collet@unistra.fr, jparmspach@unistra.fr

The paper is organized as follows. Section II describes the methods. In section III, results obtained on 3D brain images are shown. The paper finishes with conclusions.

II. METHOD

A. Spatio-temporal Hidden Markov Chain

The use of the Hidden Markov Chain (HMC) model to perform spatial regularization during the segmentation is a well known process [5]. In [6] Benmiloud *et al.* propose a Hidden Markov Chain model, which performs both temporal and spatial regularization. This model is suitable to our problem: the cerebral structures that we want to segment (WM, GM, CSF) exhibit a spatial consistency over time. HMC requires a vector in input, so the first step is to transform two 3D images into a vector. In this goal, a 3D+t Hilbert-Peano scan is used (Fig. 1). A different 4D HMC model can be found in [7]. To a 3D segmentation by Markov Random Field, this model add a temporal Markov chain in each voxel.

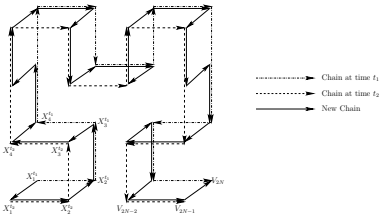

Fig. 1. 3D+t Hilbert-Peano scan.

Let us consider two random processes at time t_1 and at time t_2, $X^{t_i} = (X_n^{t_i})_{n\in S}$ standing for hidden processes and $\boldsymbol{Y}^{t_i} = (\boldsymbol{Y}_n^{t_i})_{n\in S}$ the observed ones, with $i = \{1, 2\}$ the process associated with image at time t_1 and at time t_2 respectively and the finite set of N voxels on the 3D lattice S. Each $X_n^{t_i}$ takes its value in finite set of $K = 3$ classes $\Omega = \{\omega_{CSF}, \omega_{GM}, \omega_{WM}\}$. Each $\boldsymbol{Y}_n^{t_i}$ takes its value in $\mathbb{R}^m$ with m the number of MRI modalities (the modalities should be T1, T2, Flair). Let us define $X = [X_1^{t_1}, X_1^{t_2}, X_2^{t_2}, X_2^{t_1}, X_3^{t_1}, \ldots, X_{N-1}^{t_2}, X_N^{t_2}, X_N^{t_1}]$. To introduce a spatio-temporal regularization in the segmentation process we assume that X is a Markov Chain then $P(X_{n+1} = \omega_l | X_n = \omega_k, \ldots, X_1 = \omega_j) = P(X_{n+1} = \omega_l | X_n = \omega_k)$. Thus X will be determined by an initial probability $\pi_k = P(X_1^{t_1} = \omega_k)$ and the spatial transition matrices:

$$\begin{cases} \boldsymbol{A}^{t_1,n} : a_{kl}^{t_1,n} = P(X_{n+1}^{t_1} = \omega_l | X_n^{t_1} = \omega_k) \\ \boldsymbol{A}^{t_2,n} : a_{kl}^{t_2,n} = P(X_{n+1}^{t_2} = \omega_l | X_n^{t_2} = \omega_k) \end{cases} \quad (1)$$

978-1-4244-7929-0/14/$26.00 ©2014 IEEE

and the temporal transition matrix $\boldsymbol{T}^n$ with elements $t^n_{kl} = P(X^{t_i}_n = \omega_l | X^{t_{\bar{i}}}_n = \omega_k)$ (with $\bar{i} = 2$ $(resp.\ 1)$ if $i = 1$ $(resp.\ 2)$). We assume homogeneity of the Markov Chain which means that the transition matrices are independent of the location n: $a^{t_1,n}_{kl} = a^{t_1}_{kl}$, $a^{t_2,n}_{kl} = a^{t_2}_{kl}$, $t^n_{kl} = t_{kl}$. The spatio-temporal Hidden Markov Chain scheme is presented in Fig. 2.

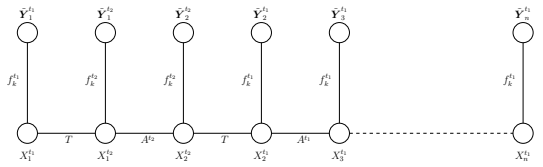

Fig. 2. Spatio-temporal Hidden Markov Chain.

MR images are corrupted with inhomogeneity, which can lead misclassifications in the segmentation process. To correct this bias field, we use the method introduced by Van Leemput *et al.* [8], in which the bias field is modeled as a linear combination $\sum_l \boldsymbol{b}^{t_i}_l \phi_l(n)$ of polynomial basis functions $\phi_l(n)$. Inhomogeneities being multiplicative, we take the logarithm of the observations in order to have an additive bias. Let us define the bias corrected intensity $\tilde{\boldsymbol{Y}}^{t_i}_n = \log(\boldsymbol{Y}^{t_i}_n) - \sum_l \boldsymbol{b}^{t_i}_l \phi_l(n)$. The estimation of the bias parameters $\boldsymbol{b}^{t_i}_l$ is done following a weighted least-squares scheme [8].

For each image, the likelihood

$$f^{t_i}_k(\tilde{\boldsymbol{y}}^{t_i}_n; \theta^{t_i}_k) = p(\tilde{\boldsymbol{Y}}^{t_i}_n = \tilde{\boldsymbol{y}}^{t_i}_n | X^{t_i}_n = \omega_k) \tag{2}$$

stands for the data driven term which is assumed to follow multivariate normal distribution with the mean $\boldsymbol{\mu}^{t_i}_k$ and the covariance matrix $\boldsymbol{\Sigma}^{t_i}_k$. The estimation of these parameters $\theta^{t_i}_k = \{\boldsymbol{\mu}^{t_i}_k, \boldsymbol{\Sigma}^{t_i}_k\}$, as the estimation of *prior* parameters $\theta_{HMC} = \{\boldsymbol{\pi}, \boldsymbol{A}^{t_1}, \boldsymbol{A}^{t_2}, \boldsymbol{T}\}$ are described in the next section.

The two segmented images are obtained by using the MPM (Mode of Posterior Marginals) estimator [9]: $\hat{x}_n = \arg\max_{\omega_k} P(X_n = \omega_k | \boldsymbol{Y} = \boldsymbol{y})$, maximizing the *a posteriori* probabilities in every node of the 4D chain. One of the main advantages of HMC compared to Markov Random Field is that the *posterior* probabilities can be computed exactly at each voxel, as shown in the following. That allows to reduce the computation time (no MCMC sampling required) and to still keep sufficient spatial information [10].

B. Chain Parameters Estimation

The Baum-Welch algorithm [4] allows us to estimate the *posterior* probabilities needed to calculate the segmentation criterion and to update the HMC model parameters θ_{HMC} and the noise parameters $\theta^{t_i}_k$. In this iterative algorithm, the *posterior* probabilities estimation and the HMC model parameters and the noise parameters are estimated sequentially. To have a fully unsupervised method, the whole parameters are initialized using a K-means segmentation [11]. Let us define:

$$V = [X^{t_1}_1, X^{t_2}_1, X^{t_2}_2, X^{t_1}_2, X^{t_1}_3, \ldots, X^{t_2}_{N-1}, X^{t_2}_N, X^{t_1}_N] \tag{3}$$

$$\boldsymbol{Z} = [\tilde{\boldsymbol{Y}}^{t_1}_1, \tilde{\boldsymbol{Y}}^{t_2}_1, \tilde{\boldsymbol{Y}}^{t_2}_2, \tilde{\boldsymbol{Y}}^{t_1}_2, \tilde{\boldsymbol{Y}}^{t_1}_3, \ldots, \tilde{\boldsymbol{Y}}^{t_1}_N] \tag{4}$$

$$d^n_{kl} = P(V_{n+1} = \omega_l | V_n = \omega_k) \tag{5}$$

$$[g_k(\tilde{\boldsymbol{y}}^{t_1}_1), \ldots, g_k(\tilde{\boldsymbol{y}}^{t_1}_N)] = [f^{t_1}_k(\tilde{\boldsymbol{y}}^{t_1}_1), f^{t_2}_k(\tilde{\boldsymbol{y}}^{t_2}_1), \ldots, f^{t_1}_k(\tilde{\boldsymbol{y}}^{t_1}_N)] \tag{6}$$

To simplify the notations, we will note $\boldsymbol{z}_n$ for $\boldsymbol{Z}_n = \boldsymbol{z}_n$ in all the notations with data (for example, the posterior probabilities $P(V_n = \omega_k | \boldsymbol{Z} = \boldsymbol{z})$ will be noted $P(V_n = \omega_k | \boldsymbol{z})$).

1) The posterior *probabilities expectation step.:* The *posterior* probabilities are estimated by scanning the chain in both directions. First the forward probabilities is estimated :

$$\begin{aligned} \alpha_n(k) &= P(V_n = \omega_k | \boldsymbol{z}_1, \ldots \boldsymbol{z}_n), \forall n \in [1, 2N] \\ &= \begin{cases} \pi_k g_k(\boldsymbol{z}_1) & \text{if } n = 1 \\ \sum_{l=1}^K \alpha_{n-1}(l) d^{n-1}_{lk} g_k(\boldsymbol{z}_n) & \text{otherwise} \end{cases} \end{aligned} \tag{7}$$

and then the backward probabilities

$$\begin{aligned} \beta_n(k) &= \frac{P((\boldsymbol{z}_{n+1}, \ldots \boldsymbol{z}_{2N}) | V_n = \omega_k)}{P((\boldsymbol{z}_{n+1}, \ldots \boldsymbol{z}_{2N}) | \boldsymbol{z}_1, \ldots \boldsymbol{z}_n)}, \forall n \in [1, 2N] \\ &= \begin{cases} 1 & \text{if } n = 2N \\ \sum_{l=1}^K \beta_{n+1}(l) d^n_{kl} g_l(\boldsymbol{z}_{n+1}) & \text{otherwise} \end{cases} \end{aligned} \tag{8}$$

Finally the *posterior* probability is calculated [9]: $P(V_n = \omega_k | \boldsymbol{z}) = \alpha_n(k)\beta_n(k), \forall k \in [1, K]$.

2) θ_{HMC} and $\theta^{t_i}_k$ estimation step.: In the second step, the HMC model parameters and the noise parameters are estimated using the forward and the backward probabilities in a maximum likelihood scheme. Let us define the *a posteriori* joint probabilities $P(V_n = \omega_l, V_{n-1} = \omega_k | \boldsymbol{z}) = \xi_{n-1}(k, l) = \alpha_{n-1}(k) d^{n-1}_{kl} g_l(\boldsymbol{z}_n) \beta_n(l)$ and the *a posteriori* marginal probabilities $P(V_n = \omega_k | \boldsymbol{z}) = \gamma_n(k) = \alpha_n(k)\beta_n(k)$. The HMC model parameters are then estimated:

$$\pi_k = \gamma_1(k) \tag{9}$$

$$a^{t_1}_{kl} = \frac{\sum_{n=1}^{N/2-1} \xi_{4n+1}(k, l)}{\sum_{n=1}^{N/2-1} \gamma_{4n+1}(k)} \tag{10}$$

$$a^{t_2}_{kl} = \frac{\sum_{n=1}^{N/2} \xi_{4n-1}(k, l)}{\sum_{n=1}^{N/2} \gamma_{4n-1}(k)} \tag{11}$$

$$t_{kl} = \frac{\sum_{n=1}^{N} \xi_{2n}(k, l)}{\sum_{n=1}^{N} \gamma_{2n}(k)} \tag{12}$$

and the noise parameters:

$$\boldsymbol{\mu}^{t_i}_k = \frac{\sum_{n \in t_i} \gamma_n(k) \boldsymbol{z}_n}{\sum_{n \in t_i} \gamma_n(k)} \tag{13}$$

$$\boldsymbol{\Sigma}^{t_i}_k = \frac{\sum_{n \in t_i} \gamma_n(k) (\boldsymbol{z}_n - \boldsymbol{\mu}^{t_i}_k)(\boldsymbol{z}_n - \boldsymbol{\mu}^{t_i}_k)^t}{\sum_{n \in t_i} \gamma_n(k)} \tag{14}$$

The estimation of the noise parameters may depend on artefacts or outliers such as introduce by Multiple Sclerosis lesions. To reduce this influence, we estimate the parameters in a robust way by using the Trimmed Likelihood Estimator which is introduced in the next section.

C. Trimmed Likelihood Estimator

In the Baum-Welch algorithm, the parameter $\theta = \{\theta_k^{t_i}, \theta_{HMC}\}$ is estimed by a Maximum Likelihood Estimator (MLE) method. We use Trimmed Likelihood Estimator (TLE) to estimate these parameters in a robust way, which is define as:

$$\hat{\Theta}_{TLE} = \arg\max_{\theta} \prod_{n=1}^{h} g(\boldsymbol{z}_{\nu(n)}, \theta) \tag{15}$$

where $\nu = (\nu(1), \ldots, \nu(2N))$ is a permutation of the indices sorting the data by adequacy with the model and h is the trimming parameter. MLE is a special case of TLE with $h = N$. The TLE method was first used in the context of MS lesions detection by At-Ali *et al.* [12] and adapted in the context of Hidden Markov Chain model [13]. In the estimation, this estimator discards the data $\boldsymbol{z}_n$, for which the probability $P(\boldsymbol{z}_n, \theta)$ is smaller than a threshold s.

$$\begin{aligned} P(\boldsymbol{z}_n, \theta) &= \sum_{k=1}^{K} P(\boldsymbol{z}_n, V_n = \omega_k, \theta) \\ &= \sum_{k=1}^{K} P(V_n = \omega_k) P(\boldsymbol{z}_n, \theta | V_n = \omega_k) \\ &= \sum_{k=1}^{K} P(V_n = \omega_k) g_k(\boldsymbol{z}_n, \theta) \end{aligned} \tag{16}$$

For a significant number of nodes, as $\boldsymbol{A}^{t_1}$ and $\boldsymbol{A}^{t_2}$ are in pratical almost identical and as $\boldsymbol{T}$ is almost the identity matrix, we can consider that our Hidden Markov Chain becomes time-homogeneous ($P(V_n = \omega_k)$ is constant). Then the probability $P(\boldsymbol{z}_n, \theta)$ is close in each node to an unique Gaussian Mixture Model (GMM) distribution, given by:

$$\begin{aligned} h_{MG}(\boldsymbol{z}_n, \theta) &= \sum_{k=1}^{K} \alpha_k g_k(\boldsymbol{z}_n, \theta) \\ &\approx P(\boldsymbol{z}_n, \theta) \end{aligned} \tag{17}$$

We can then determine numerically the threshold s verifying:

$$\begin{aligned} \int_{\Phi_s} h_{MG}(\boldsymbol{z}, \theta) d\boldsymbol{z} &= p_{EVT} \\ \Phi_s &= \{\boldsymbol{z} | h_{MG}(\boldsymbol{z}, \theta) \geq s\} \end{aligned} \tag{18}$$

where p_{EVT} is a probability chosen by the user. The trimming parameter h is then defined by $h = card(\boldsymbol{z}_n \in \Phi_s)$.

The data disgarded are considered as outliers. From this outliers, we keep as MS lesions the blob which size is superior to $3mm^3$ and which distance from the edge of the brain is enough (5 voxels). This post-treament reduce the one-off outliers and the outliers in CSF (in the edge of the brain), which are not MS lesions.

III. VALIDATION

To validate our spatio-temporal Hidden Markov Chain model (STHMC), in particular the contribution of the temporal dimension, we compare the MRI brain segmentation with our method and with a classical Hidden Markov Chain methods [13]. For the tests, we use the Brainweb Database [1] [14], which propose different phantoms of brain MRI with different levels of noise (from 0% to 9%), different levels of inhomogeneity (from 0% to 40%) and different lesion load. From this phantoms the ground truth is known. To compare the performance of the two algorithms, we use the Kappa index (KI):

$$KI = 2\frac{SEG \cap GT}{SEG + GT} \tag{19}$$

where GT stands for ground truth and SEG for the obtained segmentation.

A. Tests on BrainWeb images without MS lesions

The method was first tested on T1/T2 images with 20% inhomogeneity for different levels of noise, without lesions. We choise an inhomogeneity of 20% corresponding to realistic case nevertheless, this level have weak influence on the results. The results are shown in Tab.I. For the spatio-temporal method, the two different times used different levels of noise. For this method, the mean and the variation of KI obtained for different noise combinations are presented. With our method, the mean Kappa index is always higher than 95% for all levels of noise and for all brain structures. Segmentation of all brain structures obtained with our method is always better than the classical HMC method. These results confirm the interest of using a time neighbourhood information for the brain structures segmentation. The spatio-temporal regularization provided by our STHMC model during the segmentation process allow a reduction of the noise effects: results change little despite the increase of the noise.

TABLE I

RESULTS OBTAINED ON BRAINWEB IMAGES WITHOUT MS LESIONS WITH 20% INHOMOGENEITY FOR DIFFERENT LEVEL OF NOISE. KAPPA INDEX (KI) IS REPORTED FOR WHITE MATTER (WM), GRAY MATTER (GM) AND CEREBROSPINAL FLUID (CSF) FOR THE CLASSICAL HIDDEN MARKOV CHAIN ALGORITHM (HMC) AND FOR OUR METHOD (STHMC)

noise	method	CSF	GM	WM
1%	HMC	95.1	95.8	96.4
	STHMC	96.1 ± 0.2	96.5 ± 0.6	97.0 ± 0.8
3%	HMC	94.9	94.1	93.7
	STHMC	95.8 ± 0.2	95.5 ± 0.4	95.7 ± 0.5
5%	HMC	94.1	93.8	94.0
	STHMC	95.6 ± 0.5	95.5 ± 1.0	95.9 ± 1.1
7%	HMC	93.0	92.9	93.4
	STHMC	95.4 ± 0.8	95.3 ± 1.2	95.8 ± 1.4
9%	HMC	91.8	91.7	92.6
	STHMC	95.3 ± 0.7	95.1 ± 1.2	95.5 ± 1.4

B. Tests on BrainWeb images with MS lesions (same lesion load)

The second series of test were done on T1/T2 images with MS lesions (a "mild" lesion load). The other conditions remain the same. The results are shown in Tab. II.

[1] http://www.bic.mni.mcgill.ca/brainweb/

Despite less successful results than in the case without MS lesions, our method still provides a good segmentation of brain structures in the presence of MS lesions, which shows the efficiency of the Trimmed Likelihood Estimator. Moreover our method obtain better results than the classical HMC method for the segmentation of brain structures. For the segmentation of MS lesions, the results are equivalent for both methods.

TABLE II

RESULTS OBTAINED ON BRAINWEB IMAGES WITH MS LESIONS WITH 20% INHOMOGENEITY FOR DIFFERENT LEVEL OF NOISE. KAPPA INDEX (KI) IS REPORTED FOR WHITE MATTER (WM), GRAY MATTER (GM), CEREBROSPINAL FLUID (CSF) AND MS LESIONS (MS) FOR THE CLASSICAL HIDDEN MARKOV CHAIN ALGORITHM (HMC) AND FOR OUR METHOD (STHMC)

noise	method	CSF	GM	WM	MS
1%	HMC	82.1	89.4	93.8	67.9
	STHMC	92.34 ± 1.7	93.1 ± 0.5	94.0 ± 1.5	72.0
3%	HMC	83.9	88.9	92.7	77.2
	STHMC	92.3 ± 1.5	93.1 ± 0.4	94.2 ± 1.3	78.5
5%	HMC	88.1	88.5	91.5	78.2
	STHMC	92.2 ± 1.2	93.1 ± 0.3	94.4 ± 1.0	77.6
7%	HMC	88.4	87.4	90.2	58.0
	STHMC	92.1 ± 0.5	92.9 ± 0.5	94.1 ± 1.2	53.5

C. Tests on BrainWeb images with MS lesions (different lesion load)

Finally, we test our method on T1/T2 images with MS lesions. The lesion load in the image at first time is "mild" whereas the lesion load in the image at the second time is "severe". The results are show in Tab. III.

Even in a presence of temporal evolution (a change in a lesion load), our method have better results than the classical HMC method for the segmentation of brain structures and equivalent results for the segmentation of MS lesions. This validate the contribution of the temporal dimension in the segmentation of structures.

TABLE III

RESULTS OBTAINED ON BRAINWEB IMAGES WITH MS LESIONS WITH 20% INHOMOGENEITY FOR DIFFERENT LEVEL OF NOISE AND DIFFERENT LESION LOAD. KAPPA INDEX (KI) IS REPORTED FOR WHITE MATTER (WM), GRAY MATTER (GM), CEREBROSPINAL FLUID (CSF) AND MS LESIONS (MS) FOR THE CLASSICAL HIDDEN MARKOV CHAIN ALGORITHM (HMC) AND FOR OUR METHOD (STHMC)

case	method	CSF	GM	WM	MS
3%	HMC	83.9	88.9	92.7	77.2
mild	STHMC	88.1	91.5	94.0	82.5
3%	HMC	83.8	85.5	90.1	82.0
severe	STHMC	85.8	90.0	93.0	82.7
5%	HMC	88.1	88.5	91.5	78.2
mild	STHMC	89.7	92.3	94.5	78.0
5%	HMC	84.8	85.5	89.4	82.4
severe	STHMC	87.1	90.8	93.6	81.4
7%	HMC	88.4	87.4	90.2	58.0
mild	STHMC	90.8	92.3	93.8	54.4
7%	HMC	85.0	84.8	88.4	73.1
severe	STHMC	88.1	91.0	91.3	71.9

IV. CONCLUSION

In this paper, we have introduced and validated a robust method for simultaneously segmenting the tissues of two brain MR images. We used a spatio-temporal Hidden Markov Chain to take into account both spatial and temporal neighbourhood information during the segmentation process in the way to reduce the influence of the noise present in MR images. To improve the robustness, in particular in the present of modified brain tissues such as MS lesions, we use Trimmed Likelihood Estimator. After a post-treament, we use the outliers define by the TLE to determine MS lesions. This method was tested on 3D brain MRI phantoms with and without MS lesions.

REFERENCES

[1] J. S. Suri, S. Sameer, and L. Reden, "Computer vision and pattern recognition techniques for 2-d and 3-d MR cerebral cortical segmentation: A state-of-the-art review," *Pattern Analysis and applications*, vol. 5, pp. 46–98, 2002.

[2] D. Mortazavi, A. Z. Kouzani, and H. Soltanian-Zadeh, "Segmentation of multiple sclerosis lesions in MR images: a review," *Neuroradiology*, vol. 54, pp. 299–320, 2012.

[3] X. Lladó, A. Oliver, M. Cabezas, J. Freixenet, J. C. Vilanova, A. Quiles, L. Valls, L. Ramió-Torrentà, and A. Rovira, "Segmentation of multiple sclerosis lesions in brain MRI: A review of automated approaches," *Information Sciences*, vol. 186, no. 1, pp. 164–185, 2012.

[4] L. E. Baum, T. Petrie, G. Soules, and N. Weiss, "A maximization technique occurring in the statistical analysis of probabilistic functions of Markov chains," *The Annals of Mathematical Statistics*, vol. 41, no. 1, pp. 164–171, 1970.

[5] N. Giordana and W. Pieczynski, "Estimation of generalized multisensor hidden markov chains and unsupervised image segmentation," *IEEE Transactions on Pattern Analysis and Machine Intelligence*, vol. 19, no. 5, pp. 465–475, 1997.

[6] B. Benmiloud and W. Pieczynski, "Estimation des paramètres dans les chaînes de Markov cachées et segmentation d'images," *Traitement du Signal*, vol. 12, no. 5, pp. 465–475, 1995.

[7] J. Solomon, J. A. Butman, and A. Sood, "Segmentation of brain tumors in 4D MR images using the hidden Markov model," *Computer Methods and Programs in Biomedicine*, vol. 84, pp. 76–85, 2006.

[8] K. Van Leemput, F. Maes, D. Vandermeulen, and P. Suetens, "Automated model-based bias field correction of MR images of the brain," *IEEE Transactions On Medical Imaging*, vol. 18, no. 10, pp. 885–896, 1999.

[9] A. Gelman, J. B. Carlin, H. S. Stern, D. B. Dunson, A. Vehtari, and D. B. Rubin, *Bayesian data analysis*. Chapman & Hall/CRC, 2013.

[10] F. Salzenstein and C. Collet, "Fuzzy Markov random fields versus chains for multispectral image segmentation," *IEEE Transactions on Pattern Analysis and Machine Intelligence*, vol. 28, pp. 1753–1767, 2006.

[11] S. Bricq, C. Collet, and J.-P. Armspach, "Unifying framework for multimodal brain MRI segmentation based on hidden Markov chains," *Medical Image Analysis*, vol. 12, no. 6, pp. 639–652, 2008.

[12] L. S. At-Ali, S. Prima, P. Hellier, B. Carsin, G. Edan, and C. Barillot, "Strem: a robust multidimensional parametric method to segment MS lesions in MRI," in *Medical Image Computing and Computer-Assisted Intervention*, 2005, pp. 409–416.

[13] S. Bricq, C. Collet, and J.-P. Armspach, "Lesions detection on 3D brain MRI using trimmmed likelihood estimator and probabilistic atlas," in *Biomedical Imaging: From Nano to Macro, 2008. ISBI 2008. 5th IEEE International Symposium on*, 2008.

[14] R. K.-S. Kwan, A. C. Evans, and G. B. Pike, "An extensible MRI simulator for post-processing evaluation," in *Visualization in Biomedical Computing*, ser. Lecture Notes in Computer Science, K. Höhne and R. Kikinis, Eds. Springer Berlin Heidelberg, 1996, vol. 1131, pp. 135–140. [Online]. Available: http://dx.doi.org/10.1007/BFb0046947